Test of ITER-TF Joint Samples With NIFS Test Facilities

Test of ITER-TF Joint Samples With NIFS Test Facilities

Shinsaku Imagawa, *Member, IEEE*, Hideki Kajitani, Tetsuhiro Obana, Suguru Takada, Shinji Hamaguchi, Hirotaka Chikaraishi, *Member, IEEE*, Kazuya Takahata, Kunihiro Matsui, Tsutomu Hemmi, and Norikiyo Koizumi

***Abstract*—Qualification tests of the ITER toroidal field (TF) conductor joints have been carried out by testing joint samples with test facilities in the National Institute for Fusion Science, NINS, Toki, Japan. The joint sample consists of two short TF conductors with the length of 1535 mm, which is restricted by the test facility with 9-T split coils and 100-kA current leads. The sample current is supplied from a dc 75-kA power supply. Each conductor has two joint boxes at both terminals. The lower joint is a testing part that is a full-size joint of the TF coil. The joint resistance of the lower joint is estimated from the increase of the average voltage drop among the six taps on the conductor against the currents. Five joint samples were tested until 2016, and all the samples satisfied the requirement of the joint resistance at less than 3 nΩ. The method of the measurement and the results are summarized, and the voltage distribution among the voltage taps is discussed.**

***Index Terms*—Cable-in-conduit, current distribution, ITER TF coil, joint resistance.**

I. Introduction

EACH Toroidal Field (TF) coil of ITER contains seven double-pancakes that are electrically connected each other with "twin-box" joints [1]–[4]. The twin-box joint is also adopted for the TF coil terminal. The twin-box joint was firstly developed at CEA Cadarache (France) for Cable-In-Conduit (CIC) conductors [5]. The low electrical resistance in nΩ is attained by the direct contact of the superconducting strands pressed to the copper sleeve of the box and by soldering of adjacent copper sleeve of the two boxes [6], [7]. The required joint resistance of the ITER-TF conductor joints is less than 3 nΩ at 2 T background field.

Qualification tests of the ITER TF conductor joints have been carried out prior to manufacture of each TF coil by testing each short joint sample with test facilities in National Institute for Fusion Science. Five joint samples were tested until 2016, and all the samples satisfied the requirement. In this paper, the method of the measurement and the experimental results are summarized, and the voltage distribution among the voltage taps is discussed.

Manuscript received August 26, 2017; accepted November 11, 2017. Date of publication November 16, 2017; date of current version December 1, 2017. This work was supported in part by the Grants-in-Aid from MEXT, in part by the collaborative research with the Mitsubishi Electric Corporation and the Toshiba Corporation, and in part by the NIFS Collaboration Research program under Grant ULAA003. *(Corresponding author: Shinsaku Imagawa.)*

S. Imagawa, T. Obana, S. Takada, S. Hamaguchi, H. Chikaraishi, and K. Takahata are with the National Institute for Fusion Science, National Institutes of Natural Sciences, Toki 509-5292, Japan (e-mail: imagawa@LHD.nifs.ac.jp).

H. Kajitani, K. Matsui, T. Hemmi, and N. Koizumi are with the Fusion Energy Research and Development Directorate, National Institute for Quantum and Radiological Science and Technology, Naka 311-0193, Japan.

Color versions of one or more of the figures in this paper are available online at http://ieeexplore.ieee.org.

Digital Object Identifier 10.1109/TASC.2017.2774368

II. Test Facility and Setup of Samples

A. Test Facilities

A conductor testing facility with 9 T split-type coils is used for testing the joint samples. The coils are composed of NbTi and Nb3Sn superconductors and operated in liquid helium [8]. The inner and outer diameters of the coil are 248 and 907 mm, respectively, and the cross-section of a sample bore is 100 mm wide and 550 mm long. The effective length of the magnetic field higher than 95% of the maximum is ±100 mm from the center axis. The sample current is supplied from a dc 75 kA power supply that is composed of three 25 kA unit banks to reduce ripples of the output voltage [9]. The current stability is within ±0.75%, and the deviation of the measured current from the setting current is less than ±1% in the short circuit test. The maximum ramp rate is 999 A/s. The vapor-cooled current leads can carry a continuous 40 kA current, and the current carrying of 75 kA for 10 min has been confirmed [10].

The sample data are acquired with a VXI Bus mainframe (Agilent E8404A) that includes a 64-channel scanning A/D converter (Agilent E1413C) with the functions of low-pass filters and input amplifiers. The scanned data are converted to physical quantities using a workstation and saved as readable output files.

B. Specification of Samples

An ITER-TF conductor consists of six petals of multi-twisted strands wrapped with stainless steel tapes, a center channel, and a conduit [7]. The total numbers of Nb3Sn and copper strands are 900 and 522, respectively. The joint sample consists of two short TF conductors with the length of 1,535 mm, which is restricted by the conductor test facility with the 9 T split coils. Each conductor has two joint boxes at both terminals. The joint box consists of a copper sleeve, twin boxes, and a cover, as shown in Fig. 1. The lower joint is a testing part that is a full size joint of the TF coil, where the strands are contacted to the copper sleeve by the length of 440 mm, the same as the final twisting pitch length of the cable. The total length of the lower joint box is 675 mm including the transition region of cable compaction. In order to attain the original conductor part of

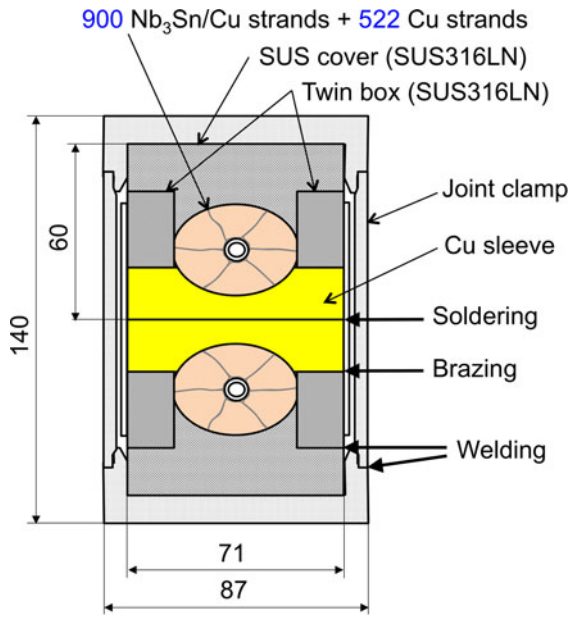

Fig. 1. Schematic drawing of cross-section of an ITER-TF joint box.

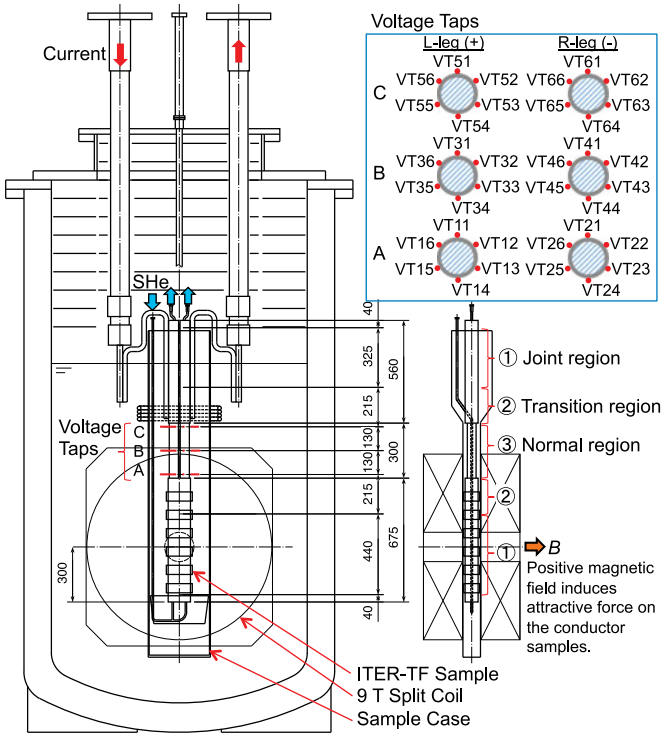

Fig. 2. A setup of an ITER-TF joint sample in the 9 T test facility.

300 mm length for setting voltage taps at three positions, the length of the upper joint box is shortened to 560 mm, where the joint length of the cable and the copper sleeve is shortened to 325 mm, as shown in Fig. 2.

At the joint region, a cable wrap and sub-cable wraps at the outer surface of the cable are removed, and the chromium layer of the cable surface is also removed [5]. The cable is compacted from the void fraction of 33% to 25%. Good electrical and mechanical connection between the cable and the copper sleeve

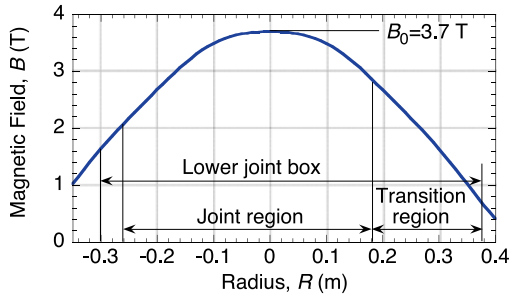

Fig. 3. Magnetic field distribution at the central field of 3.7 T.

is achieved by sintering through heat treatment of the sample. The copper sleeves of the lower joint are connected to one another using PbSn solder.

C. Setup of Samples

The upper terminals of the joint sample are attached to copper bus-bars in which superconducting wires are buried to reduce heat generation. The bus-bars are attached to the current leads, and the whole assembly is installed into the 9 T test facility. The lower joint is set near the center of the split coils. At the central field, B_0 of 3.7 T, the lowest field in the joint region is higher than 2.0 T, as shown in Fig. 3.

While the 9 T split coils of the test facility are cooled with liquid helium, the CIC conductor sample is cooled with supercritical helium (SHe). Therefore, a sample case made from stainless steel is inserted between the split coils. The samples are tested in gaseous helium atmosphere. This method was developed for testing CIC conductors for JT-60SA [11], [12]. SHe is supplied from a helium refrigerator through a heat exchanger that is immersed in liquid helium. The cooling pipe at the inlet is equipped with film heaters to control the SHe temperature from 4 K to 6 K.

Voltage taps are attached on the conduit surface at three longitudinal positions in the normal conductor region, as shown in Fig. 2. In order to cancel the voltage distribution due to non-uniform currents, star voltage taps are adopted, and the joint resistance is evaluated by averaging their values.

III. Experimental Results

A. Experimental Methods

The 9 T split coils are cooled with liquid helium at 0.12 MPa, and the joint sample in the sample case is cooled with SHe at the pressure of 0.5 MPa and at the flow rate of around 3 g/s. The sample is cooled down together with the split coils in approximately 30 hours from room temperature to 4 K. The temperature of supplied gaseous helium is gradually lowered. After the split coils are immersed with liquid helium, the SHe flow rate of the sample is adjusted.

Before excitation of the split coils, the inlet temperature of the sample is set. Next, the split coils are charged to the testing field, which is held for more than 600 s to reduce the shielding currents induced in the sample. After that, the sample is charged up to the nominal current of 68 kA with holding the current for 300 s

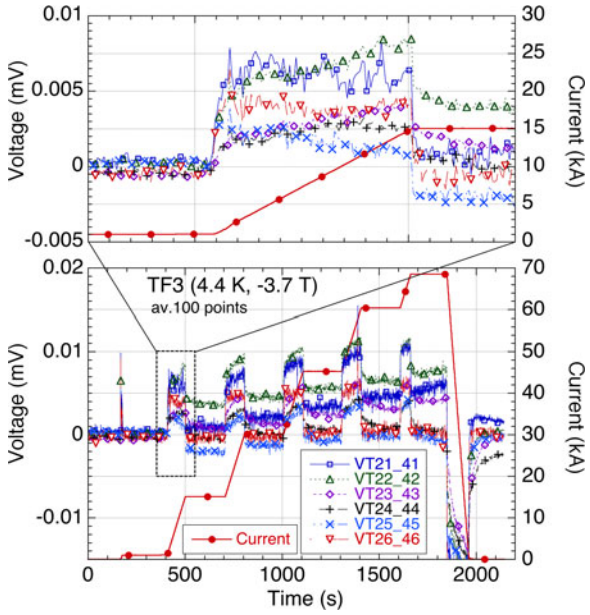

Fig. 4. Longitudinal voltage drops in R-leg of the 3rd joint sample at the external field of −3.7 T at 4.4 K.

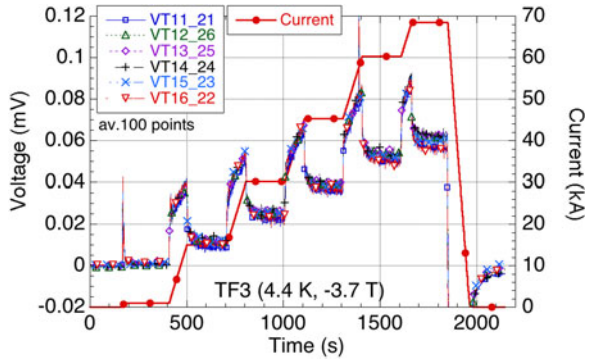

Fig. 5. Voltages across the lower joint at the position A of the 3rd sample at the external field of −3.7 T at 4.4 K.

at 1 kA, 15 kA, 30 kA, 45 kA, 60 kA, and 68 kA to eliminate the effect of shielding currents. The charging rate is 150 A/s, and discharging is 600 A/s. The external field and the inlet temperature of the sample are kept constant during charging the sample. A pair of voltage taps to measure the joint resistance is set to be across the lower joint at the same vertical position, such as VT11 and VT21. In addition, the voltage drops in the R-leg are measured with pairs of taps in neighbor vertical positions, such as VT21 and VT41. All voltage signals are recorded at intervals of 0.01 s.

B. Voltage Distribution and Joint Resistance

The typical experimental data for the longitudinal voltage drops are shown in Fig. 4, and the voltages across the lower joint are shown in Fig. 5. In order to cancel the noises coming mainly from the power supply, all data are averaged for 1 s, which corresponds to 100 data points. Each voltage is offset by each average value for 30 s just before charging. The difference among the six longitudinal voltage drops is within 0.01 mV,

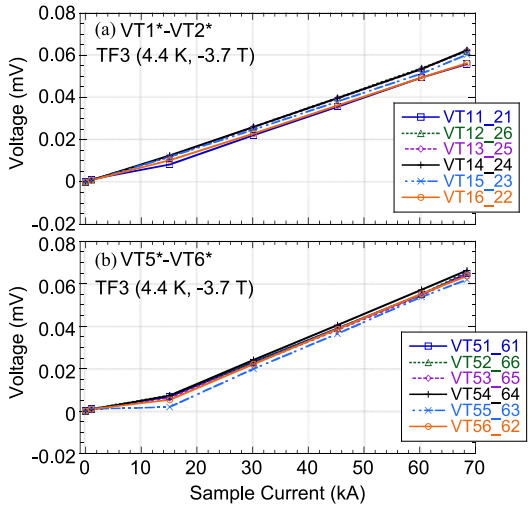

Fig. 6. Voltages averaged for last 30 s in each period of holding current at the positions A (a) and C (b) of the 3rd joint sample at −3.7 T at 4.4 K.

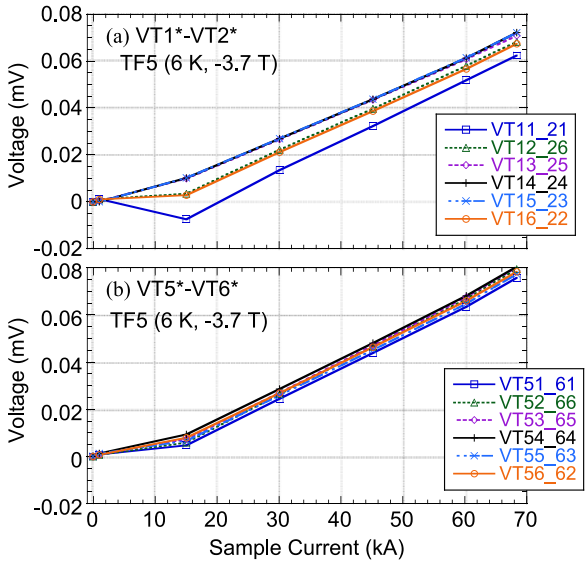

Fig. 7. Voltages averaged for last 30 s in each period of holding current at the positions A (a) and C (b) of the 5th joint sample at −3.7 T at 6 K.

which is the same as the voltages across the joint. The difference in the longitudinal voltage drops is enlarged to 0.01 mV at less than 15 kA and saturated at the higher currents. In the case of Fig. 4, the drift of the voltages seems to have occurred from 5 kA to 10 kA. Positive voltage rise of 0.002–0.005 mV/60 kA at the currents higher than 15 kA is considered to be caused by the currents in the conduit, because the conduit is directly contacted to the joint boxes [7], [13]. The current flowing pattern in the strands of the sample should be changed between 1 kA and 15 kA.

The joint resistance is estimated from the incline of the regression line of the average voltages versus the current. The voltages across the lower joint are averaged for the last 30 s in each 300 s of holding the current. Their typical results are shown in Figs. 6(a), (b), and 7(a), (b). In the case of Fig. 7(a), the difference among the six voltages is enlarged to 0.02 mV at less than 15 kA and gradually reduced at the higher current. In

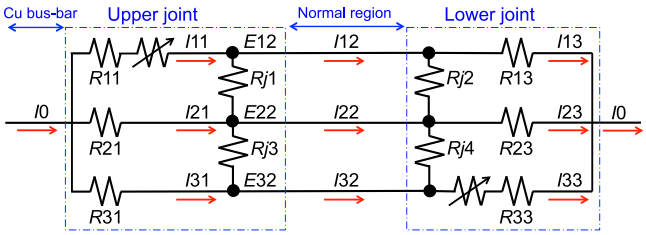

Fig. 8. Simplified electric circuit model for one leg of a joint sample. The upper (or lower) line corresponds to a strand that is contacted with a low resistance to the copper sleeve of the upper (or lower) joint, and the middle line corresponds to the other strands.

all cases, the average voltages except for those at 0 and 1 kA are well fitted by linear lines. Since the voltages after discharge recover to zero, the drift of signals by the amplifiers should be small. Therefore, the voltage rises at the current less than 15 kA is considered to be small. The tendency is clearer at the voltage taps in the positions B and C in Fig. 2. The similar phenomena are observed in all five samples. The joint resistances, estimated from data except for at 0 and 1 kA, of the five sample are 1.1, 2.9, 1.0, 0.91, 1.1 nΩ at B_0 of −3.7 T and at 4.4 K as the average among the data at the three positions.

IV. Discussion

The voltage distribution in CIC conductors has been studied by many scientists, and a few dynamic simulation codes to solve currents in the strands have been developed [14]–[16]. In order to understand the non-linear behavior of the voltages in joint samples at the low current less than 15 kA, we consider a simplified electric circuit model, as shown in Fig. 8, that represents one conductor of the joint sample. This model can simulate the case that the current of one strand in the upper and/or lower joint exceeds the critical current, I_c. Since this model consists of only resistors, the solution can be derived analytically. *R*11 to *R*33 are the joint resistances between strands and the copper sleeve of the joint box. Here, *R*11 and *R*33 are set at low resistances to simulate non-uniform currents. If the current *I*11 (or *I*33) exceeds I_c, *I*11 (or *I*33) is fixed at I_c, and *R*11 (or *R*33) is changed to a variable. The middle line in Fig. 8 corresponds to the other strands (898 Nb3Sn strands), and *R*21 and *R*23 are set at 0.5 nΩ, which is one-half of the typical joint resistance of the joint samples. *Rj*1, *Rj*2, *Rj*3, and *Rj*4 are the interstrand contact resistances, which is reported in the range of 10 nΩ [17]. The current transfer during the normal region is ignored because of high interstrand contact resistance there [15].

In this study, I_c of the strand is set at 1 kA, and *R*13 and *R*31 are set at 450 nΩ, which is the typical joint resistance per strand. In addition, *Rj*1, *Rj*2, *Rj*3, and *Rj*4 are set at the same value, *Rj*. By these assumptions, *I*33 depends mainly on *R*33 and *Rj*. In the case that both *R*11 and *R*33 are extremely low, both *I*11 and *I*33 exceed I_c, and *E*12 becomes higher than the average and saturated, as shown in Fig. 9(a), the tendency of which seems different from the experiment. In the case that *I*11 does not exceed I_c, the calculated results are similar to the experiment, as shown in Fig. 9(b) and (c). The maximum difference among the voltages is mainly dependent on *Rj*. In the case that *R*33 is

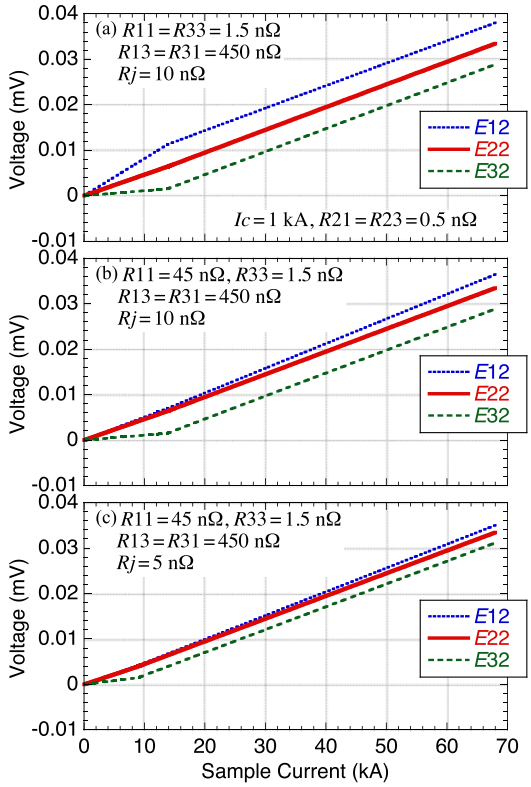

Fig. 9. Calculated results with the circuit in Fig. 8 for different *R*11 and *Rj*.

1/300 of the average and *Rj* of 5 nΩ, the voltage difference of 0.01 mV and its saturation at the current less than 10 kA can be simulated. In reality, the interstrand contact resistances are varied, and few strands should reach I_c from the strand jointed to the copper sleeve with the lower resistance and with lower interstrand contact resistances.

Since *E*22 corresponds to the average voltage, this model can not simulate the clearly low average resistance at low currents. Further research is necessary to explain this phenomenon as well as the difference in the tap positions.

V. Conclusion

The measurement of joint resistance in nΩ has been carried out for ITER-TF conductors by using the conductor test facility with 9 T split coils and the dc 75 kA power supply. The necessary accuracy is attained by adopting star voltage taps and by averaging large data collected with 100 Hz sampling. All the five samples satisfied the requirement of the joint resistance less than 3 nΩ at 2 T. The difference among the voltages of the six taps is enlarged to the range of 0.01 mV and saturated at the current less than 15 kA. A simplified electric circuit model is proposed, and the saturation of differences among the voltage taps at the current around 10 kA can be simulated by the assumption of existence of a strand contacted to the copper sleeve with a extremely low joint resistance.

Acknowledgment

The views and opinions expressed herein do not necessarily reflect those of the ITER Organization.

REFERENCES

[1] C. Sborchia, Y. Fu, R. Gallix, C. Jong, J. Knaster, and N. Mitchell, "Design and specifications of the ITER TF coils," *IEEE Trans. Appl. Supercond.*, vol. 18, no. 2, pp. 463–466, Jun. 2008.

[2] K. Matsui, T. Hemmi, H. Kajitani, K. Takano, M. Yamane, and N. Koizumi, "Progress of ITER TF coil development in Japan," *IEEE Trans. Appl. Supercond.*, vol. 24, no. 3, Jun. 2014, Art. no. 4203105.

[3] N. Koizumi *et al.*, "Progress in procurement of ITER toroidal field coil in Japan," *IEEE Trans. Appl. Supercond.*, vol. 26, no. 4, Jun. 2016, Art. no. 4203004.

[4] T. Hemmi *et al.*, "Development of ITER toroidal field coil in Japan," *IEEE Trans. Appl. Supercond.*, vol. 27, no. 4, Jun. 2017, Art. no. 4200105.

[5] P. Decool *et al.*, "Joints for large superconducting conductors," *Fusion Eng. Des.*, vol. 58/59, pp. 123–127, 2001.

[6] B. Stepanov, P. Bruzzone, S. March, and K. Sedlak, "Twin-box ITER joints under electromagnetic transient loads," *Fusion Eng. Des.*, vol. 98/99, pp. 1158–1162, 2015.

[7] H. Kajitani *et al.*, "Evaluation of ITER TF coil joint performance," *IEEE Trans. Appl. Supercond.*, vol. 25, no. 3, Jun. 2015, Art. no. 4202204.

[8] J. Yamamoto *et al.*, "Superconducting test facility of NIFS for the large helical device," *Fusion Eng. Des.*, vol. 20, pp. 147–151, Jan. 1993.

[9] S. Yamada *et al.*, "Characteristics of a dc 75 kA power supply in the superconducting magnet test facilities," *Fusion Eng. Des.*, vol. 20, pp. 201–209, Jan. 1993.

[10] T. Mito *et al.*, "Development of 100 kA current leads for superconductor critical current measurement," *Fusion Eng. Des.*, vol. 20, pp. 217–222, Jan. 1993.

[11] T. Obana *et al.*, "Upgrading the NIFS superconductor test facility for JT-60SA cable-in-conduit conductors," *Fusion Eng. Des.*, vol. 84, no. 7–11, pp. 1442–1445, Jun. 2009.

[12] T. Obana *et al.*, "Conductor and joint test results of JT-60SA CS and EF coils using the NIFS test facility," *Cryogenics*, vol. 73, pp. 25–41, Jan. 2016.

[13] N. Koizumi *et al.*, "Experimental results at pulse test facility (PTF) of butt joint used in ITER CS model coil outer module," in *Proc. 17th Int. Conf. Cryogenic Eng.*, 1998, pp. 523–526.

[14] Y. Ilyin, A. Nijhuis, and H. H. J. Ten Kate, "Interpretation of conduit voltage measurements on the poloidal field insert sample using the CUDI-CICC numerical code," *Cryogenics*, vol. 46, pp. 517–529, 2006.

[15] N. Koizumi, K. Matsui, and K. Okuno, "Analysis of current and voltage distribution in the first Japanese qualification sample of an ITER TF conductor," *Cryogenics*, vol. 50, pp. 129–138, Mar. 2010.

[16] E. P. A. van Lanen and A. Nijhuis, "Jackpot: A novel model to study the influence of current non-uniformity and cabling patterns in cable-in-conduit conductors," *Cryogenics*, vol. 50, pp. 139–148, 2010.

[17] N. Koizumi *et al.*, "Critical current test results of 13 T–46 kA Nb3Al cable-in-conduit conductor," *Cryogenics*, vol. 42, pp. 675–690, 2002.